

First Records of Late Triassic Conodont Fauna and $\delta^{13}\text{C}_{\text{carb}}$ from the Dengdengqiao Section, Dangchang County, Gansu Province, Northwestern China

Hanxiao Li¹, Miao Yan Wang², Muhui Zhang^{1,3}, Paul B. Wignall⁴, Manuel Rigo⁵, Yanlong Chen⁶, Xianlang Wu¹, Zhumin Ouyang¹, Baojin Wu¹, Zhaoyang Yi⁷, Zaitian Zhang^{8,9}, Xulong Lai^{10*},^{1,3}

1. School of Earth Sciences, China University of Geosciences, Wuhan 430074, China

2. School of Earth Sciences and Resources, China University of Geosciences, Beijing 100083, China

3. State Key Laboratory of Biogeology and Environmental Geology, China University of Geosciences, Wuhan 430078, China

4. School of Earth and Environment, University of Leeds, Leeds LS2 9JT, UK

5. Department of Geosciences, University of Padova, Via Gradenigo 6, 35131, Padova, Italy

6. Shaanxi Key Laboratory of Early Life and Environments, State Key Laboratory of Continental Dynamics and Department of Geology, Northwest University, Xi'an 710069, China

7. Key Laboratory of Orogenic Belts and Crustal Evolution, School of Earth and Space Sciences, Peking University, Beijing 100871, China
8. Wuhan Center of Geological Survey, Wuhan 430205, China

9. State Key Laboratory of Palaeobiology and Stratigraphy, Nanjing Institute of Geology and Palaeontology, Chinese Academy of Sciences, Nanjing 210008, China

*Hanxiao Li: <https://orcid.org/0000-0001-6774-0618>; Xulong Lai: <https://orcid.org/0000-0002-2837-0885>

ABSTRACT: Based on a study of 49 conodont and 57 geochemical samples from the Upper Triassic, carbonate-dominated Dengdengqiao Formation, Qinling Basin, China, the Carnian conodonts and carbon isotope records are first reported. Two genera and four species have been identified amongst 87 conodont elements: *Mosherella praebudaensis*, *Mo. longnanensis* sp. nov., *Mo.* sp., and “*Misikella*” *longidentata*. The presence of *Mo. praebudaensis* indicates that the lower part (bed 2) of the formation is attributable to the Julian (lower Carnian) substage. A radiolarian fauna identified in a previous study belongs to the upper Carnian, but the sampling horizon is unclear. The $\delta^{13}\text{C}_{\text{carb}}$ curve shows a ~1.8‰ negative excursion beginning from upper part of bed 3, but its stratigraphic location is uncertain. The Dengdengqiao Formation is clearly at least partly of Carnian age but could include younger strata. The abundant calcareous algae at the section is probably due to some transport rather than preserved in site. The unusual ecosystem with rare marine organisms may reflect long-term stressful and unfavorable conditions at Dengdengqiao.

KEY WORDS: conodonts, Late Triassic, Julian, Qinling.

0 INTRODUCTION

The Late Triassic marine strata widely distributed in the western part of Qinling and adjacent areas record a key period in the evolutionary history of this region. The South China Block and North China Block merged to form the Qinling Orogenic Belt in the Late Triassic (Yang et al., 2016, 2002), resulting in the disappearance of Qinling Basin (e.g., Li et al., 2003; Lai et al., 1995, 1992; Yin et al., 1988). However, few fossils have been reported from the widely distributed Late Triassic strata in this region. Records are restricted to the radiolarian fauna recovered from the Dengdengqiao Section, Dangchang County (southern Gansu

Province) (Fig. 1), which was speculated to be of Carnian (early Late Triassic) age (Xu, 1992). In this paper, we report on a conodont fauna from the Dengdengqiao Section and provide the first reliable fossil evidence for Upper Triassic strata in the Qinling region.

Late Triassic conodonts have received much less attention compared with those of the Early or Middle Triassic (e.g., Liu et al., 2020; Chen Y et al., 2019; Chen Y L et al., 2019; Li et al., 2019; Yang et al., 2019; Lyu et al., 2018). Conodont biostratigraphy is an important tool for the subdivision and correlation of Late Triassic marine strata (e.g., Rigo et al., 2018, 2007; Zhang et al., 2018a, b; Chen and Lukeneder, 2017) thanks to the good preservational potential, wide distribution and high evolutionary rates of conodonts.

For Carnian conodonts, their P_1 elements can be roughly divided into two categories: segminate and segminiplanate. At present, Carnian conodont zones are mainly based on the segminiplanate elements belonging to *Paragondolella*, *Quadralella*,

*Corresponding author: xllai@cug.edu.cn

© China University of Geosciences (Wuhan) and Springer-Verlag GmbH Germany, Part of Springer Nature 2021

Manuscript received October 29, 2020.

Manuscript accepted February 3, 2021.

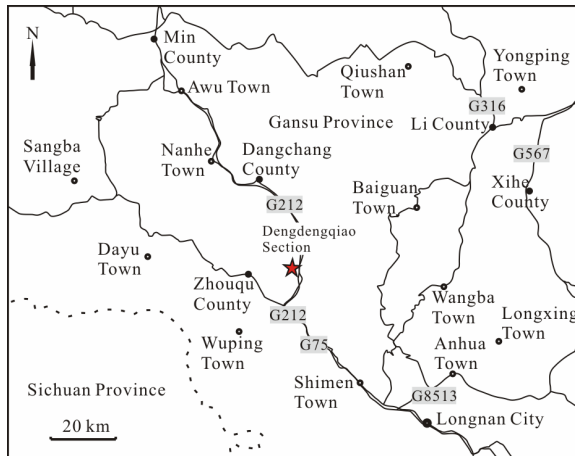


Figure 1. Present-day location of the Dengdengqiao Section indicated by the red star.

Budurovignathus, *Carnepigondolella*, *Metapolygnathus*, *Mazzaella*, *Gladigondolella*, *Kraussodontus* and *Acuminatella*. Nevertheless, their evolutionary relationships are complex (e.g., Karádi et al., 2020; Chen et al., 2016; Mazza et al., 2012a) and the base index conodont of Carnian still remains controversial. In comparison, the contemporary segminate elements of *Mosherella*, *Neocavittella* and “*Misikella*” have received much less attention. Among them, the genus *Mosherella* may have significant potential for the subdivision of Carnian strata, and the type species *Mosherella newpassensis* is a potential auxiliary index fossil for the basal Carnian (Sweet et al., 1971; Mosher, 1968).

Mosherella has been reported from North America, Europe, Turkey and Malaysia (e.g., Chen and Lukeneder, 2017; Kolar-Jurkovšek and Jurkovšek, 2010; Orchard, 2010; Orchard and Balini, 2007; Orchard and Tozer, 1997; Mosher, 1968) but in South China only segminiplanate conodonts have been

widely reported from Carnian strata (Jiang et al., 2019; Zhang et al., 2018a, b, 2017; Shi et al., 2017; Sun et al., 2016). Only a single segminate conodont specimen, attributed to *Mosherella*, is known from the Guandao Section, Nanpanjiang Basin (the same materials were listed in Lehrmann et al., 2015 and Wang et al., 2005). Here, the discovery of *Mosherella* in South Qinling increases the occurrence of this genus, and provides us an opportunity to study it in detail.

1 GEOLOGICAL SETTING AND STRATIGRAPHY

The Dengdengqiao Section is located in the Dangchang County, Gansu Province, northwestern China (Fig. 1, start point GPS 33.844°N, 104.542°E, height 1 597 m a.s.l.). The Dangchang area belongs to the South Qinling belt (Dong et al., 2015), and was situated in the east part of the Qinling Basin in the Late Triassic (Fig. 2).

The Triassic strata can be subdivided into six formations in Dangchang (Lai, 1992), in ascending order, they are Maresongduo Formation (T_1m), Guojiashan Formation (T_2g), Qinyu Formation (T_2q), Huashiguan Formation (T_2h), Dengdengqiao Formation (T_3dd), and Daheba Formation (T_3dh). These formations have conformable contacts, except for the Dengdengqiao and Daheba formations which have a tectonic contact (Lai, 1992). The Maresongduo Formation is mainly characterized by thick-bedded dolomite or dolomitic limestone. The Guojiashan Formation mostly consists of thick-bedded micritic limestone and bioclastic limestone with an abundant Anisian fauna including conodonts, bivalves, brachiopods, gastropods and ammonoids. The succeeding Qinyu Formation is composed of shales, siltstone and micritic limestone with banded chert and has a bivalve and conodont fauna indicating a Ladinian age. The overlying Huashiguan Formation is comprised of thin-bedded, carbonaceous slates, calcareous siltstone, shale, micritic limestone and slump breccias and lacks

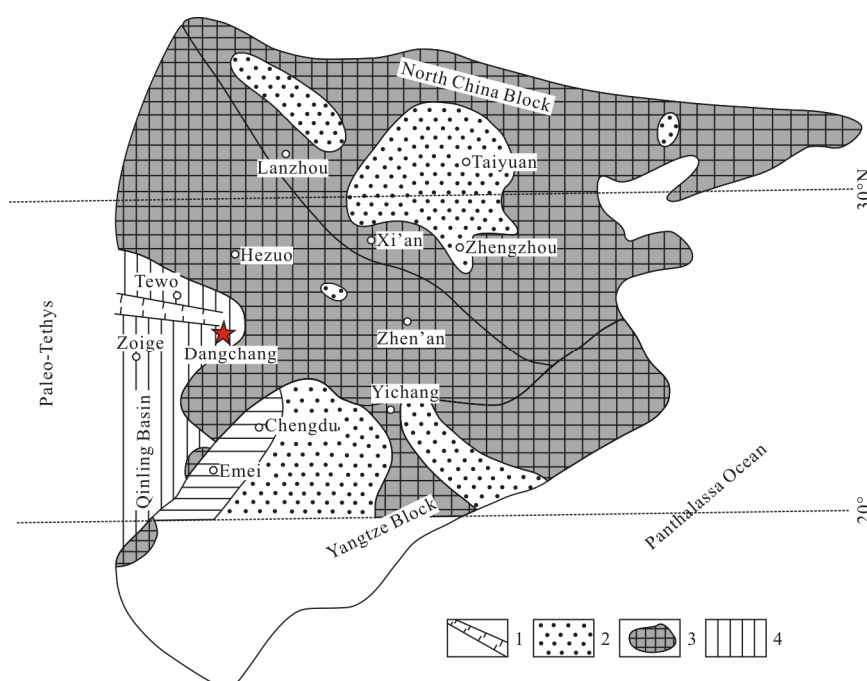


Figure 2. Paleoceanographic reconstruction of Qinling area in early Late Triassic. 1. Center of an aulacogen; 2. terrestrial deposition; 3. oldlands; 4. ocean floor (modified from Lai et al., 1995, 1992).

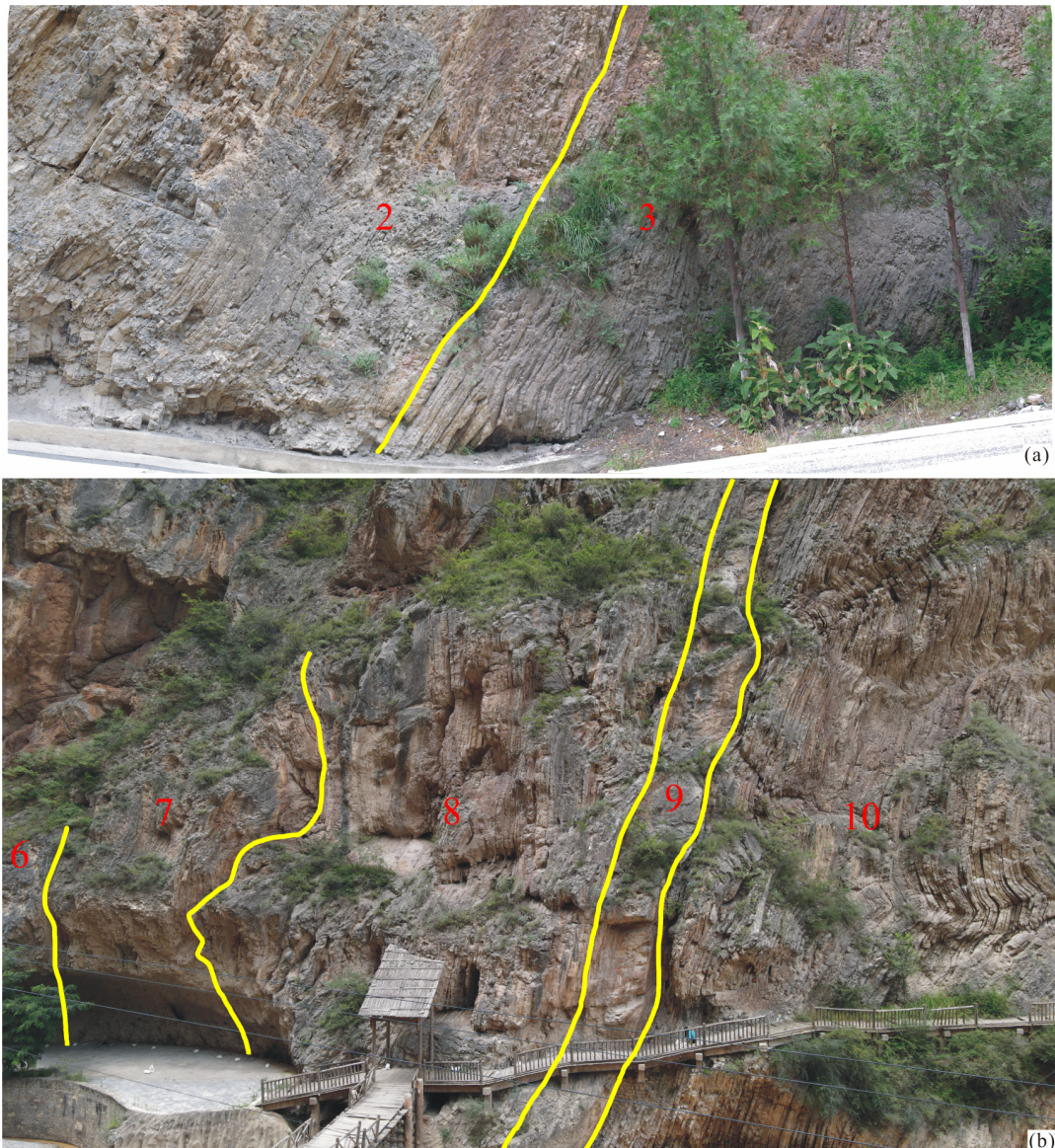


Figure 3. Outcrop photographs of Dengdengqiao Formation. (a) Thin-bedded, with a few medium-bedded, micritic limestone of beds 2–3; (b) medium- to thick-bedded micritic limestone of beds 6–10, including a 3 m thick, massive layer (bed 9).

fossils. The studied Dengdengqiao Formation is about 400 m thick and mainly composed of thin to thick-bedded micritic limestone with abundant calcareous algae, radiolarians, and a few foraminifers, brachiopods and ostracods (Figs. 3 and 4). The Daheba Formation, the youngest marine deposits in Dangchang, is mainly represented by thick-bedded calcareous siltstone, silty shale, and thin-bedded micritic limestone, shale and mudstone. Some plant fossil fragments and pollen fossils were documented from this formation (Lai, 1992).

2 MATERIALS AND METHODS

In total, 49 conodont samples (about 4–5 kg per sample), 57 geochemical samples and 200 rock samples for thin sections were collected at Dengdengqiao (Fig. 5). The samples are indicated by the abbreviation DDQ and the corresponding meters refer to height above the base of the measured section. Conodont samples were dissolved in a 10% solution of acetic acid. The residues were then separated using an LST-an inorganic heavy

liquid (Yuan et al., 2015). Afterwards, the conodonts were collected using a stereoscopic binocular microscope and photographed using a scanning electron microscope (SEM). All specimens are stored, and all experiments were carried out, in the School of Earth Sciences, China University of Geosciences (Wuhan). Most samples were barren. However, 87 conodont elements have been obtained from 9 samples, among which only 2 samples contain P_1 elements (15 in total) (Fig. 5, Pl. 1). Two genera and four species were identified, including a new species: *Mosherella longnanensis* sp. nov. All conodonts are very small, and have very low conodont alteration indexes (CAI=1–2).

Geochemical samples were collected from fresh parts of the rock, avoiding weathered surfaces, veins of calcite and fossils, using an electric drill. The resultant ~2–3 g of powders were sent to the State Key Laboratory of Biogeology and Environmental Geology, China University of Geosciences (Wuhan) and analyzed using a MAT-253 mass spectrometer with standard methodology (see Song et al., 2013). Isotopic values are shown as per mil

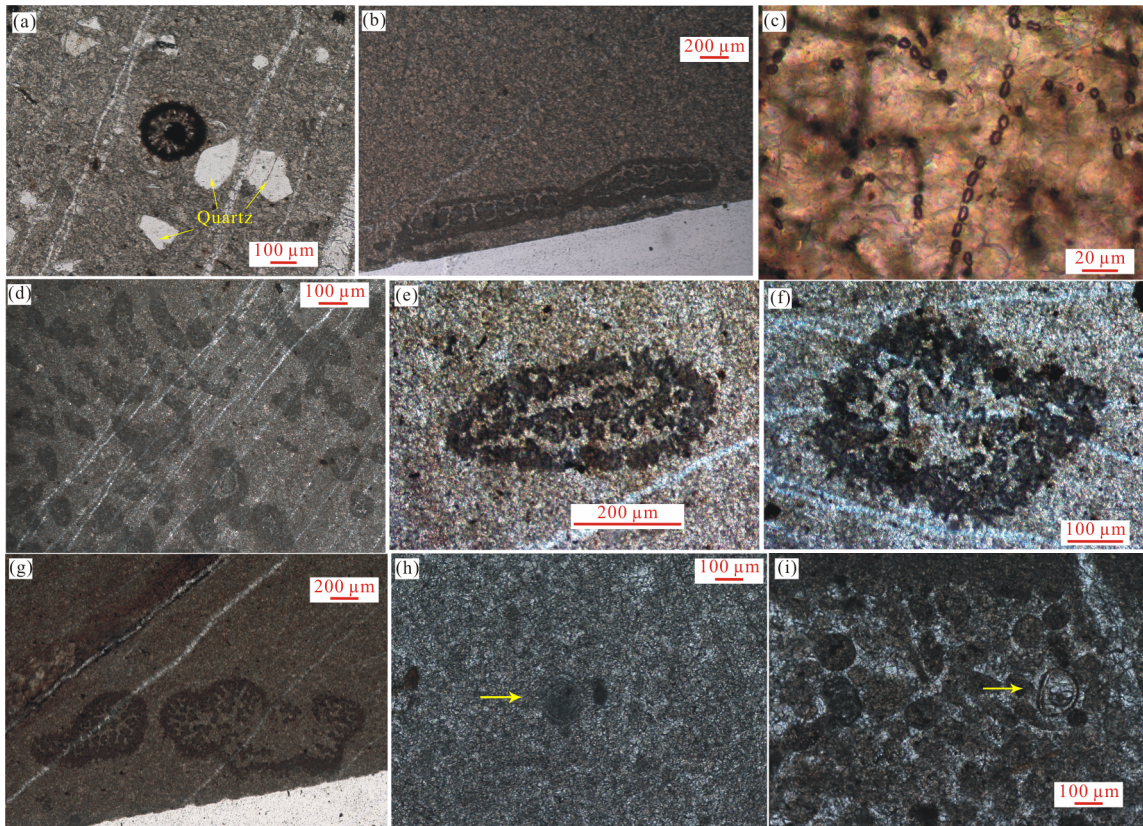


Figure 4. Photomicrographs of thin sections from Dengdengqiao Section. (a)–(g) Algae fragments in fossiliferous micrite, (a) arrows indicate quartz grains, from sample DDQ-5, bed 1, (b) from sample DDQ-69.5, bed 3, (c) from sample DDQ-70, bed 3, (d) from sample DDQ-177, bed 7, (e)–(f) from sample DDQ-189, bed 8, (g) from sample DDQ-226, bed 10; (h) fossiliferous micrite, arrow indicates foraminifer, from sample DDQ-194, bed 8; (i) sparse biomicrite, arrow indicates ostracod, from sample DDQ-139.5, bed 3. Scale bar=100 μm in (a) (f) (h) (i), scale bar=200 μm in (b) (d) (e) (g), scale bar=20 μm in (c).

relative to the Vienna Pee Dee belemnite (VPDB) standard and the analytical precision was better than $\pm 0.1\text{\textperthousand}$ and $\pm 0.2\text{\textperthousand}$ for $\delta^{13}\text{C}$ and $\delta^{18}\text{O}$, respectively.

The rock samples thin sections were made at the Langfang Geological Services Company. Petrographic analyses and photographing were carried out using a polarizing microscope (Zeiss Axioscope A1) in School of Earth Sciences, China University of Geosciences (Wuhan).

3 CONODONT FAUNA

At Dengdengqiao, *Mosherella praebudaensis*, *Mo. longnanensis* sp. nov. and *Mosherella* sp. were recovered from the upper part of bed 2 (sample DDQ-32.5), and “*Misikella*” *longidentata* was recovered from the lower part of bed 10 (sample DDQ-212.8) around 180 m higher in the section (Fig. 5).

The genus *Mosherella*, including the species *Mo. praebudaensis*, *Mo. newpassensis*, *Mo. postkockeli* and *Mo.?* *budaensis* have been reported from the Middle-Late Triassic transition to the middle Carnian (Chen et al., 2016). *Mo. postkockeli* and *Mo.?* *budaensis* were previously assigned to the genus *Nicarella* (e.g., Kolar-Jurkovšek and Jurkovšek, 2010; Kozur, 1993; Kozur and Mock, 1991), but are now suggested to belong to the genus *Mosherella* because there is >5 Ma long interval between the occurrences of the two genera (Chen et al., 2016). The genus *Mosherella* is known from North America (Orchard, 2010; Orchard and Balini, 2007; Orchard and Tozer, 1997; Mosher, 1968), Europe (Kolar-Jurkovšek and Jurkovšek, 2019, 2010; Kozur,

1993; Kozur and Mock, 1991), southern Turkey (Chen and Lukeneder, 2017) and Malaysia (Ishida and Hirsch, 2011). In South China, one *Mo. newpassensis* specimen was found in the *Budurovignathus mungoensis* Zone at Guandao in the late Ladinian (Lehrmann et al., 2015; Wang et al., 2005). The species *Mo. praebudaensis* recovered from the upper part of bed 2 at Dengdengqiao Section was previously reported from southern Turkey (Chen and Lukeneder, 2017) and Nevada, USA (Orchard and Balini, 2007; Mosher, 1968) in Julian 2 (early Carnian) strata. So the presence of *Mo. praebudaensis* fauna at Dengdengqiao indicates a Julian (early Carnian) age, and can be correlated with the UA2 or UA3 zones of the Taurus Mountains, southern Turkey (Table 1, Chen and Lukeneder, 2017).

“*Misikella*” *longidentata* was considered to belong to a different clade from the late Norian-Rhaetian *Misikella* species, and it was suggested that it should be excluded from the genus *Misikella* (Karádi et al., 2020; Fähræus and Ryley, 1989). It has a worldwide distribution and was reported from the lower Carnian to lower Norian strata in Nevada, USA (Orchard and Balini, 2007), Canada (Orchard, 2014, 1991), Sicily, Italy (Karádi et al., 2013; Mazza et al., 2012b), southern Slovakia (Channell et al., 2003), Cyprus (Fähræus and Ryley, 1989; Ryley, 1987), southern Turkey (Chen and Lukeneder, 2017) and Sichuan, China (Tian et al., 1983). This suggests that the upper part of the Dengdengqiao Formation is also of Late Triassic age, although the precise age is unknown.

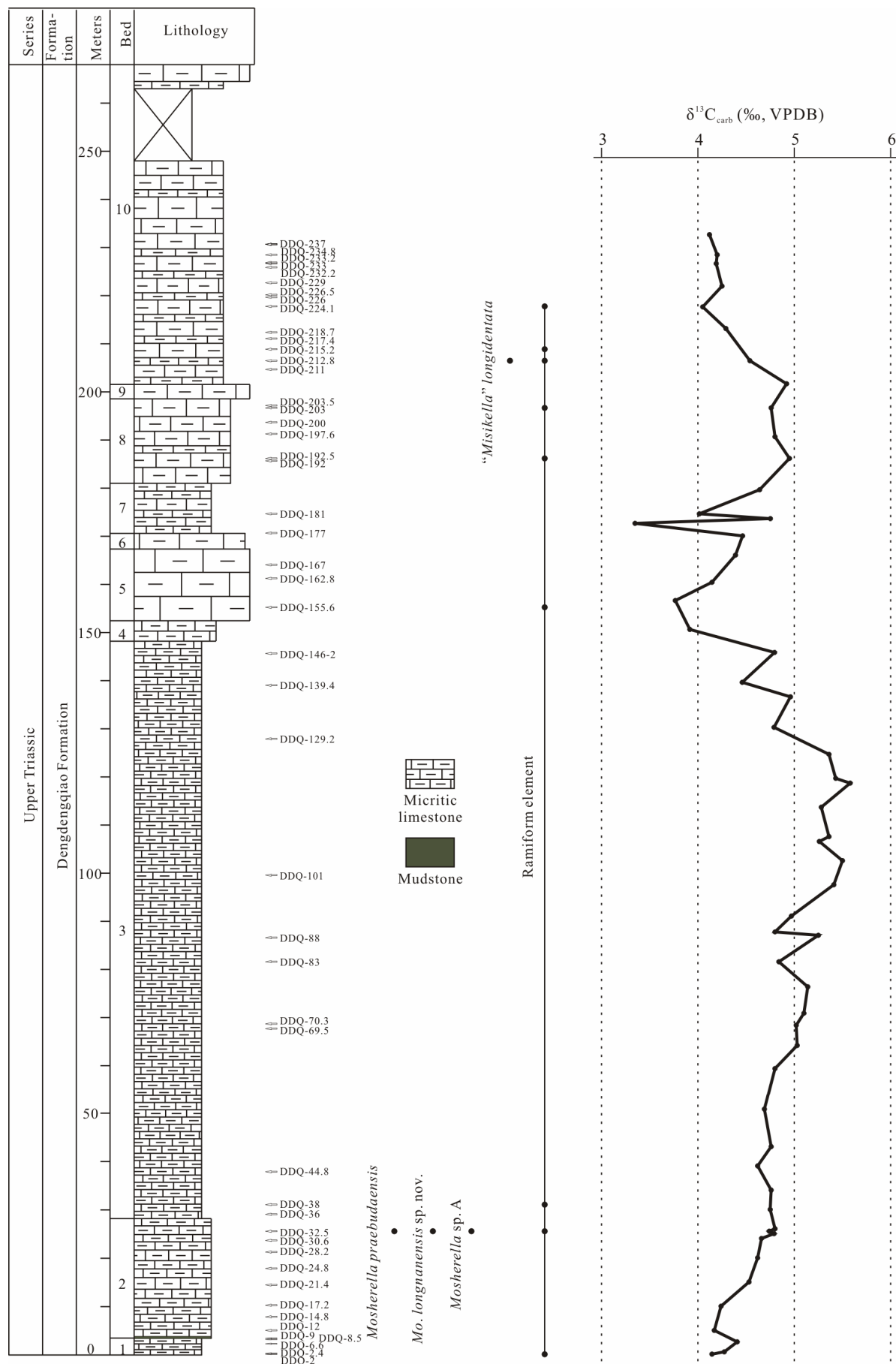


Figure 5. Conodont distribution and carbon isotopes in the Upper Triassic strata at Dengdengqiao Section, Dangchang, northwestern China.

Table 1 The correlation of the Ladinian-Carnian conodont biostratigraphy amongst different places. *A. Acuminatella*; *B. Budurovignathus*; *C. Carnepigondolella*; *E. Epigondolella*; *G. Gladigondolella*; *K. Kraussodonotus*; *M. Mazzaelia*; *Me. Metapolygnathus*; *Mo. Mositherella*; *P. Paragondolella*; *Ps. Psendojurnitius*; *Q. Quadratella*; *U. A.* unitary association. Data derived from Rigo et al. (2018); Zhang et al. (2018a); Chen and Lukenseder (2017); Balini et al. (2010); Kožar (2003); Galli et al. (1994).

		Ammonoid zones		Conodont zones or fauna					
Stage	Location	Tethyan (Balini et al., 2010)	Alps (Gallet et al., 1994)	Western Tethys (Rigo et al., 2018)	North America (Kozur, 2003)	Southwestern China (Zhang et al., 2018a)	Southern Turkey (Chen and Lukeneder, 2017)	Slovenia (Kolar-Jurkoviček and Jurkovšek, 2019)	Dangchang, South Qinling (this paper)
Substage									
Ladinian	Longobardian	Tuvalian							
		Anatropites spinosus	<i>Q. nodosa</i>	<i>E. vialovi</i>	<i>E. primitia</i>			<i>E. rigoi-</i> <i>E. quadrata</i>	
				<i>C. orchardi</i>	<i>Me. communisti</i>			<i>C. pseudodiebeli-</i> <i>C. zoae</i>	
				<i>Ne. cavitata</i>	<i>C. zoae</i>				
		Tropites subbulatus	<i>Q. carpathica</i>	<i>Me. praecommunis</i>	<i>C. lindae</i>	<i>Q. ex gr. carpathica</i>		<i>Q. tuvalica</i>	
			<i>Q. polygnathiformis</i>	<i>H. n. sp.</i>	<i>H. tuvalica</i>	<i>Q. noah</i>		<i>Q. carpathica</i>	
		Tropites dilieri							
		Austrotrachyceras austriacum		<i>G. tethydis</i>	<i>P. praelindae</i>			<i>Mo. ? budapestensis</i>	
								<i>Mo. ? budapestensis</i>	
		Trachyceras aonoides	<i>Q. auriformis</i>	<i>Ma. carnica</i>	<i>Q. polygnathiformis</i>			<i>Mo. praebudapestensis</i>	
		Trachyceras aon	<i>Q. tadpole</i>	<i>Q. polygnathiformis</i>				<i>Mo. postkockeli-</i>	
		Daxatina canadensis	<i>B. mostleri</i>					<i>K. praeargustus-</i>	
								<i>P. inclinata-</i>	
		Frankites regoledanus	<i>B. diebeli</i>					<i>Q. polygnathiformis</i>	
									<i>Q. polygnathiformis</i>
									<i>P. foliata</i>
									<i>B. mungoensis</i>
									<i>P. s. murcitanus</i>

4 CARBON ISOTOPE RECORD

The geochemical samples from Dengdengqiao are mostly fresh with well-preserved sedimentary textures. The average values of $\delta^{13}\text{C}$ and $\delta^{18}\text{O}$ are +4.7‰ and -4.7‰, respectively and show very weak correlation (Fig. 6). In addition, the conodont alteration index (CAI=1–2) is very low, indicating modest burial depths. Based on these observations, we consider that the carbon isotope record at Dengdengqiao Section is likely to be an original signal.

The $\delta^{13}\text{C}_{\text{carb}}$ values increase slowly from +4.2‰ at the base of the section to +5.6‰ in the upper part of bed 3 (Fig. 5). This is followed by a gradual decline of values that culminates in a low point at the base of bed 5 of +3.8‰, before values rise again to +4.5‰ in bed 6. A second, sharper negative excursion occurs in bed 7 (values fall to +3.4‰) before values gradually rise to nearly +5‰. Finally, $\delta^{13}\text{C}_{\text{carb}}$ values gradually fall again to +4.1‰ in bed 10.

5 DISCUSSION

5.1 Age of Dengdengqiao Formation

The conodonts from the Dengdengqiao Section indicate that the lower part (bed 2) of the section belongs to the Julian (lower Carnian) substage. In a previous study, a radiolarian fauna was recovered from the middle or upper part of Dengdengqiao Formation, but the exact sampling position is unclear (Xu, 1992). The radiolarian fauna includes *Acanthosphaera* sp., *Archaeospongoprunum collare*, *Betraccium* sp., *Cenosphaera marginata*, *C.* sp., *Flustrella* sp., *Liosphaeridae* gen. indet., *Monostylosphaera sinensis*, *Pantanellium* sp., *Sepsagon?* *spiralis*, *Spongostaurus* sp., *Stylosphaera* sp., *Spumellarina* spp., *Stauracontium* sp. These taxa suggested a Carnian (early Late Triassic) age according to Xu (1992). O'Dogherty et al. (2010) summarized the biostratigraphy of Triassic radiolarians, and noted that the genus *Betraccium* ranged from the late Carnian to Rhaetian, the genus *Pantanellium* ranged from the late Carnian to Jurassic, and the genus *Monostylosphaera* only occurred in the Carnian. These ranges suggest the upper part of Dengdengqiao Formation is probably of late Carnian or potentially younger age.

Correlation using the $\delta^{13}\text{C}_{\text{carb}}$ curve is rendered difficult because of the lack of biostratigraphic markers in the middle or

upper part of Dengdengqiao Formation. It can be noted that the Carnian carbon isotopic record from Longchang, Guizhou Province (Sun et al., 2016) bears some comparison with the Dengdengqiao values. The Julian 2–early Tuvalian (mid Carnian) interval at Longchang shows a prolonged low point of $\delta^{13}\text{C}$ values that coincides with the Carnian Humid Episode, a major climatic event, and is similar to that seen in the upper part of bed 3–bed 7 at Dengdengqiao. However, the overall values of $\delta^{13}\text{C}_{\text{carb}}$ at the latter location are some 2‰ heavier and confirmation of this correlation requires further age-diagnostic criteria.

5.2 Paleoenvironmental Analysis

The Dengdengqiao Formation is composed of dark grey, micritic limestone and a 5 cm thick grey mudstone bed between bed 1 and bed 2 (Figs. 3 and 5). The lower part of the formation (beds 1–4) is mostly thin-bedded with a few medium-bedded layers, and the upper part (beds 5–10) is mainly medium- to thick-bedded but includes a 3 m thick, massive layer (bed 9). Poorly sorted and highly angular quartz grains occur at the base of Dengdengqiao Formation (bed 1), recording a brief clastic input phase (Fig. 4a). Abundant calcareous algae were observed in the whole formation (Fig. 4), and a few foraminifers, brachiopods and ostracods were found in several thin sections.

In the previous studies, the Dengdengqiao Formation was considered to be a deep basinal facies because of the presence of radiolarians (Lai, 1992; Xu, 1992). Here we note that the general rarity of fossils suggests harsh depositional conditions, perhaps due to low oxygen levels at the seafloor. The presence of a few calcareous algae potentially indicates a shallow water, sunlit environment, but is likely that they were transported from shallow water into the basin. In addition, the foraminifers found in Dengdengqiao Formation, from samples DDQ-25 (bed 2), DDQ-162 (bed 5), DDQ-179 (bed 7), DDQ-194 (bed 8) were rare and only simple, compressed flattened forms (Fig. 4f). These small, likely opportunistic species are interpreted to be indicative of unfavorable environments (e.g., low oxygen levels) (e.g., Bernhard, 1986).

6 SYSTEMATIC PALEONTOLOGY

Mosherella longnanensis sp. nov. Li and Lai

Plate 1. 1–4

Etymology: Dengdengqiao Section, Longnan City, the type locality.

Holotype: Pl. 1.2, registration No. DDQ20032.5002

Paratype: Pl. 1.1, registration No. DDQ20032.5001

Type locality and horizon: Dengdengqiao Section, sample DDQ-32.5 in the upper part of bed 2, Dengdengqiao Formation, Dangchang, northwestern China in Julian, early Carnian, Late Triassic.

Diagnosis: A segminate P_1 element has about 8–9 posteriorly inclined, moderately to largely fused denticles. The basal cavity is expanded, oval or subrounded in shape and is located at the posterior end of the element. The posterior margin of basal cavity is rounded or blunt. The cusp is the largest denticle and it is posteriorly followed by a single tiny one.

Description: In lateral view, the species is a bladelike P_1 element, the length: height ratio is about 2 : 1. It has 8–9 moderately to largely fused denticles. The first one or two denticles

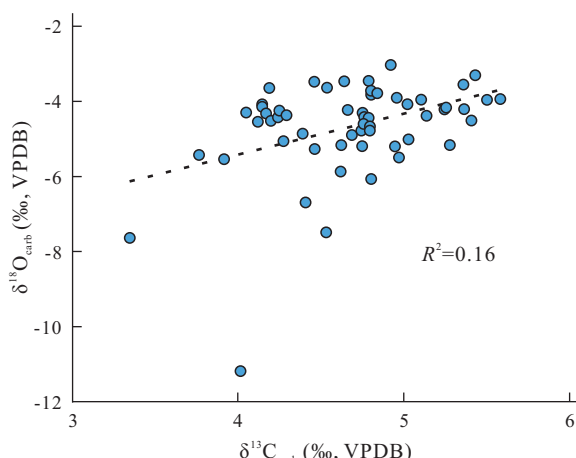


Figure 6. Crossplot of $\delta^{18}\text{O}_{\text{carb}}$ vs. $\delta^{13}\text{C}_{\text{carb}}$.

on the anterior end are erect, and then are increasingly inclined toward the posterior end of the element. The largest denticle (cusp) is the second one from posterior end, and is wider and higher than other denticles. The terminal denticle on the posterior end is much smaller than the cusp. The lower margin of the basal cavity is straight or slightly downward curved. In the lower view, the basal cavity is slightly to moderately expanded, oval or subrounded in shape, and is posteriorly located with the widest part close to the posterior end. The posterior margin of basal cavity is rounded or blunt. The basal groove develops from a small pit in the basal cavity and extends to the anterior end of the element.

Remarks: This species can be distinguished from *Mo. postkockeli*, *Mo. newpassensis* and *Mo. praebudaensis* by its rounded or blunt posterior margin of basal cavity, which is similar to middle Carnian *Mo.? budaensis*. In addition, *Mo. longnanensis* sp. nov. has a larger, posteriorly located basal cavity compared with *Mo. postkockeli* and *Mo. newpassensis*. Also, in contrast with *Mo. praebudaensis* and *Mo.? budaensis*, it has longer blade with more denticles, particularly a small denticle next to the cusp on the posterior end. In summary, this species has compounded characteristics of other species in this genus, and may be the key species in the evolutionary lineage.

The specimen *Mosherella* sp. (Pl. 1.9) looks like *Mo. longnanensis* sp. nov. in lateral view, but only has a basal groove in lower view. The basal cavity may be broken due to the poor preservation.

It is worth noting that this species is assigned to the genus *Mosherella* rather than *Neocavittella*, the reasons are as follows. Firstly the denticles are uniformly diverging in *Neocavittella* (Sudar and Budurov, 1979) but increasingly inclined toward the posterior end of the element in *Mosherella*, which could be easily differentiated by the denticles on the anterior blade. Secondly the basal cavity of the holotype (Pl. 1.2) is not as large and deep as that in *Neocavittella*. Since the basal cavity of *Mo. praebudaensis* ranges from small to large (Chen and Lukeneder, 2017), it is not difficult to distinguish *Mosherella* and *Neocavittella* just by the size of basal cavity.

Materials: 4 specimens

Stratigraphical distribution and age: Julian, early Carnian, Late Triassic.

7 CONCLUSIONS

Through systematic conodont sampling, two genera and four species were identified from the Dengdengqiao Formation for the first time, they are *Mosherella praebudanensis*, *Mo. longnanensis* sp. nov., *Mo.* sp. and “*Misikella*” *longidentata*. They indicate that the lower part (bed 2) of the formation is of Julian (early Carnian) age. This discovery, together with the previous record of late Carnian radiolarians in the middle or upper part of the formation, indicates that the formation is of Carnian age with possibly younger strata in the upper part.

The $\delta^{13}\text{C}_{\text{carb}}$ curve shows a ~1.8‰ negative excursion in the middle part of the Dengdengqiao Formation which may correspond to an excursion seen during the Carnian Humid Episode although this association requires further age criteria since there is no key biostratigraphic data in the middle or upper part of the section.

The rare marine organisms in the formation suggest long-term stressful and unfavorable environment in early Late Triassic of the Qinling region. The presence of calcareous algae at Dangchang was probably transported into the area from shallow water environments.

ACKNOWLEDGMENTS

This study was supported by the National Natural Science Foundation of China (Nos. 41830320, 45172002, 41661134047). The authors thank Qian Ye, Junlin Fu, Yongchao Li for their assistance during field works. And thanks also go to Prof. Haishui Jiang for the revision of the manuscript and Dr. Yan Chen for the personal communication. The final publication is available at Springer via <https://doi.org/10.1007/s12583-021-1428-9>.

Electronic Supplementary Material: Supplementary material (Table S1) is available in the online version of this article at <https://doi.org/10.1007/s12583-021-1428-9>.

REFERENCES CITED

- Balini, M., Lucas, S. G., Jenks, J. F., et al., 2010. Triassic Ammonoid Biostratigraphy: An Overview. *Geological Society, London, Special Publications*, 334(1): 221–262. <https://doi.org/10.1144/sp334.10>
- Bernhard, J. M., 1986. Characteristic Assemblages and Morphologies of Benthic Foraminifera from Anoxic Organic-Rich Deposits: Jurassic through Holocene. *Journal of Foraminiferal Research*, 16(3): 207–215. <https://doi.org/10.2113/gsjfr.16.3.207>
- Channell, J. E. T., Kozur, H. W., Sieversa, T., et al., 2003. Carnian-Norian Biomagnetostratigraphy at Silická Brezová (Slovakia): Correlation to Other Tethyan Sections and to the Newark Basin. *Palaeogeography, Palaeoclimatology, Palaeoecology*, 191(2): 65–109. [https://doi.org/10.1016/S0031-0182\(02\)006545](https://doi.org/10.1016/S0031-0182(02)006545)
- Chen, Y. L., Krystyn, L., Orchard, J. M., et al., 2016. A Review of the Evolution, Biostratigraphy, Provincialism and Diversity of Middle and Early Late Triassic Conodonts. *Papers in Palaeontology*, 2(2): 235–263. <https://doi.org/10.1002/spp2.1038>
- Chen, Y. L., Lukeneder, A., 2017. Late Triassic (Julian) Conodont Biostratigraphy of a Transition from Reefal Limestone to Deep-Water Environments on the Cimmerian Terranes (Taurus Mountains, Southern Turkey). *Papers in Palaeontology*, 3(3): 441–460. <https://doi.org/10.1002/spp2.1082>
- Chen, Y., Ye, Q., Jiang, H. S., et al., 2019. Conodonts and Carbon Isotopes during the Permian-Triassic Transition on the Napo Platform, South China. *Journal of Earth Science*, 30(2): 244–257. <https://doi.org/10.1007/s12583-018-0884-3>
- Chen, Y. L., Scholze, F., Richoz, S., et al., 2019. Middle Triassic Conodont Assemblages from the Germanic Basin: Implications for Multi-Element Taxonomy and Biogeography. *Journal of Systematic Palaeontology*, 17(5): 359–377. <https://doi.org/10.1080/14772019.2018.1424260>
- Dong, Y. P., Zhang, X. N., Liu, X. M., et al., 2015. Propagation Tectonics and Multiple Accretionary Processes of the Qinling Orogen. *Journal of Asian Earth Sciences*, 104: 84–98. <https://doi.org/10.1016/j.jseaes.2014.10.007>
- Fähraeus, L. E., Ryley, C. C., 1989. Multielement Species of *Misikella* Kozur and Mock, 1974 and *Axiotahea* n. gen. (Conodonta) from the Mamonia Complex (Upper Triassic), Cyprus. *Canadian Journal of Earth Sciences*, 26(6): 1255–1263. <https://doi.org/10.1139/e89-106>
- Gallet, Y., Besse, J., Krystyn, L., et al., 1994. Magnetostratigraphy of the Mayerling Section (Austria) and Erenkolu Mezarlik (Turkey) Section: Improvement of the Carnian (Late Triassic) Magnetic Polarity Time Scale. *Earth and Planetary Science Letters*, 125(1–4): 173–191.

- https://doi.org/10.1016/0012-821X(94)90214-3
- Jiang, H. S., Yuan, J. L., Chen, Y., et al., 2019. Synchronous Onset of the Mid-Carnian Pluvial Episode in the East and West Tethys: Conodont Evidence from Hanwang, Sichuan, South China. *Palaeogeography, Palaeoclimatology, Palaeoecology*, 520: 173–180. https://doi.org/10.1016/j.palaeo.2019.02.004
- Ishida, K., Hirsch, F., 2011. The Triassic Conodonts of the NW Malayan Kodiang Limestone Revisited: Taxonomy and Paleogeographic Significance. *Gondwana Research*, 19: 22–36. https://doi.org/10.1016/j.gr.2010.05.008
- Karádi, V., Kozur, H., Görög, Á., 2013. Stratigraphically Important Lower Norian Conodonts from the Csóvár Borehole (Csv-1), Hungary—Comparison with the Conodont Succession of the Norian GSSP Candidate Pizzo Mondello (Sicily, Italy). *New Mexico Museum of Natural History and Science Bulletin*, 61: 284–295
- Karádi, V., Cau, A., Mazza, M., et al., 2020. The Last Phase of Conodont Evolution during the Late Triassic: Integrating Biostratigraphic and Phylogenetic Approaches. *Palaeogeography, Palaeoclimatology, Palaeoecology*, 549: 109144. https://doi.org/10.1016/j.palaeo.2019.03.045
- Kolar-Jurkovšek, T., Jurkovšek, B., 2010. New Paleontological Evidence of the Carnian Strata in the Mežica Area (Karavanke Mts, Slovenia): Conodont Data for the Carnian Pluvial Event. *Palaeogeography, Palaeoclimatology, Palaeoecology*, 290(1–4): 81–88. https://doi.org/10.1016/j.palaeo.2009.06.015
- Kolar-Jurkovšek, T., Jurkovšek, B., 2019. Konodonti Slovenije (Conodonts of Slovenia). Geološki zavod Slovenije, Ljubljana. 260
- Kozur, H., 1993. *Nicoraella postkockeli* n. sp., a New Conodont Species from the Lower Carnian of Hungary. *Neues Jahrbuch für Geologie und Paläontologie Monatshefte*, 7: 405–412
- Kozur, H., 2003. Integrated Ammonoid, Conodont and Radiolarian Zonation of the Triassic. *Hallesches Jahrbuch Geowissenschaften*, B25: 49–79
- Kozur, H., Mock, R., 1991. New Middle Carnian and Rhaetian Conodonts from Hungary and the Alps. Stratigraphic Importance and Tectonic Implications for the Buda Mountains and Adjacent Areas. *Jahrbuch der Geologischen Bundesanstalt*, 134(2): 271–297
- Kozur, H., Mock, R., 1974. Zwei neue Conodonten-Arten aus der Trias des Slowakischen Karstes. *Časopis pro Mineralogii a Geologii*, 19(2): 135–139 (in German)
- Lai, X. L., 1992. Qinyu-Dengdengqiao, Daheba-Xinchengzi Section in Dangchang County, Gansu Province. In: Yin, H. F., Yang, F. Q., Huang, Q. S., et al., eds., Triassic in Qinling and Adjacent Areas. China University of Geosciences Press, Wuhan. 20–29 (in Chinese)
- Lai, X. L., Yin, H. F., Yang, F. Q., 1992. Reconstruction of the Triassic Qinling Sea. *Exploration of Geosciences*, (6): 57–64
- Lai, X. L., Yin, H. F., Yang, F. Q., 1995. Reconstruction of the Qinling Triassic Paleo-Ocean. *Earth Science*, 20(6): 648–656 (in Chinese with English Abstract)
- Lehrmann, D. J., Stephinski, L., Altiner, D., et al., 2015. An Integrated Biostratigraphy (Conodonts and Foraminifers) and Chronostratigraphy (Paleomagnetic Reversals, Magnetic Susceptibility, Elemental Chemistry, Carbon Isotopes and Geochronology) for the Permian–Upper Triassic Strata of Guandao Section, Nanpanjiang Basin, South China. *Journal of Asian Earth Sciences*, 108: 117–135. https://doi.org/10.1016/j.jseaes.2015.04.030
- Li, H. X., Jiang, H. S., Chen, Y. L., et al., 2019. Smithian Platform-Bearing Gondolellid Conodonts from Yiwagou Section, Northwestern China and Implications for Their Geographic Distribution in the Early Triassic. *Journal of Paleontology*, 93(3): 496–511. https://doi.org/10.1017/jpa.2018.93
- Li, Y. J., Zhao, R. F., Liu, Z. W., et al., 2003. Triassic Sedimentation and Basin Evolution in the Western Qinling. *Geology in China*, 30(3): 268–273 (in Chinese with English Abstract)
- Liu, S., Sun, Z. Y., Ji, C., et al., 2020. Conodont Biostratigraphy and Age of the Early Triassic Fish-Bearing-Nodule Levels from Nanjing and Jurong, Jiangsu Province, South China. *Journal of Earth Science*, 31(1): 9–22. https://doi.org/10.1007/s12583-019-1232-y
- Lyu, Z. Y., Orchard, M. J., Chen, Z. Q., et al., 2018. A Taxonomic Re-Assessment of the *Novispadodus waageni* Group and Its Role in Defining the Base of the Olenekian (Lower Triassic). *Journal of Earth Science*, 29(4): 824–836. https://doi.org/10.1007/s12583-018-0795-3
- Mazza, M., Cau, A., Rigo, M., 2012a. Application of Numerical Cladistic Analyses to the Carnian–Norian Conodonts: A New Approach for Phylogenetic Interpretations. *Journal of Systematic Palaeontology*, 10(3): 401–422. https://doi.org/10.1080/14772019.2011.573584
- Mazza, M., Rigo, M., Gullo, M., 2012b. Taxonomy and Biostratigraphic Record of the Upper Triassic Conodonts of the Pizzo Mondello Section (Western Sicily, Italy), GSSP Candidate for the Base of the Norian. *Rivista Italiana di Paleontologia e Stratigrafia*, 118(1): 85–130
- Mosher, L. C., 1968. Triassic Conodonts from Western North America and Europe and Their Correlation. *Journal of Paleontology*, 42: 895–946
- O'Dogherty, L., Carter, E. S., Gorican, S., et al., 2010. Triassic Radiolarian Biostratigraphy. In: Lucas, S. G., ed., The Triassic Timescale. *Special Publication of the Geological Society of London*, 334: 163–200. https://doi.org/10.1144/sp334.8
- Orchard, M. J., 1991. Late Triassic Conodont Biochronology and Biostratigraphy of the Kunga Group, Queen Charlotte Islands, British Columbia. In: Woodsworth, G. W., ed., Evolution and Hydrocarbon Potential of the Queen Charlotte Basin, British Columbia. *Geological Survey of Canada Paper*, 90-10: 173–193
- Orchard, M. J., 2010. Triassic Conodonts and Their Role in Stage Boundary Definition. *Geological Society, London, Special Publications*, 334(1): 139–161. https://doi.org/10.1144/sp334.7
- Orchard, M. J., 2014. Conodonts from the Carnian–Norian Boundary (Upper Triassic) of Black Bear Ridge, Northeastern British Columbia, Canada. *New Mexico Museum of Natural History and Science Bulletin*, 64: 1–139
- Orchard, M. J., Balini, M., 2007. Conodonts from the Ladinian–Carnian Boundary Beds of South Canyon, New Pass Range, Nevada, USA. *New Mexico Museum of Natural History and Science Bulletin*, 41: 333–340
- Orchard, M. J., Tozer, E. T., 1997. Triassic Conodont Biochronology, Its Calibration with the Ammonoid Standard, and a Biostratigraphic Summary for the Western Canada Sedimentary Basin. *Bulletin of Canadian Petroleum Geology*, 45(4): 675–692. https://doi.org/10.35767/gscpgbull.45.4.675
- Rigo, M., Preto, N., Roghi, G., et al., 2007. A Rise in the Carbonate Compensation Depth of Western Tethys in the Carnian (Late Triassic): Deep-Water Evidence for the Carnian Pluvial Event. *Palaeogeography, Palaeoclimatology, Palaeoecology*, 246(2–4): 188–205. https://doi.org/10.1016/j.palaeo.2006.09.013
- Rigo, M., Mazza, M., Karádi, V., et al., 2018. New Upper Triassic Conodont Biozonation of the Tethyan Realm. In: Tanner, L. H., ed., The Late Triassic World. *Topics in Geobiology*, 46: 189–235. https://doi.org/10.1007/978-3-319-68009-5_6
- Ryley, C. C., 1987. Multielement Taxonomy, Biostratigraphy, and Palaeoecology of Late Triassic Conodonts from the Mamonia Complex, Southwestern Cyprus: [Dissertation]. Memorial University of Newfoundland, St. John's, NL, Canada. 1–191

- Shi, Z., Preto, N., Jiang, H., et al., 2017. Demise of Late Triassic Sponge Mounds along the Northwestern Margin of the Yangtze Block, South China: Related to the Carnian Pluvial Phase?. *Palaeogeography, Palaeoclimatology, Palaeoecology*, 474: 247–263. <https://doi.org/10.1016/j.palaeo.2016.10.031>
- Song, H. Y., Tong, J. N., Algeo, T. J., et al., 2013. Large Vertical $\delta^{13}\text{C}_{\text{DIC}}$ Gradients in Early Triassic Seas of the South China Craton: Implications for Oceanographic Changes Related to Siberian Traps Volcanism. *Global and Planetary Change*, 105: 7–20. <https://doi.org/10.1016/j.gloplacha.2012.10.023>
- Sudar, M., Budurov, K., 1979. New Conodonts from the Triassic in Yugoslavia and Bulgaria. *Geologica Balcanica*, 9: 47–52
- Sun, Y. D., Wignall, P. B., Joachimski, M. M., et al., 2016. Climate Warming, Euxinia and Carbon Isotope Perturbations during the Carnian (Triassic) Crisis in South China. *Earth and Planetary Science Letters*, 444: 88–100. <https://doi.org/10.1016/j.epsl.2016.03.037>
- Sweet, W. C., Mosher, L. C., Clark, D. L., et al., 1971. Conodont Biostratigraphy of the Triassic. *Geological Society of America Memoirs*, 127: 441–466
- Tian, C. R., Dai, J. Y., Tian, S. G., 1983. Triassic Conodonts. In: Chengdu Institute of Geology and Mineral Resources, ed., Paleontological Atlas of Southwest China, Volume of Microfossils (Pt. 4, Micropaleontology). Geological Publishing House, Beijing. 345–398 (in Chinese)
- Wang, H. M., Wang, X. L., Li, R. X., et al., 2005. Triassic Conodont Succession and Stage Subdivision of the Guandao Section, Bianyang, Luodian, Guizhou. *Acta Palaeontologica Sinica*, 44(4): 611–626 (in Chinese with English Abstract)
- Xu, X. R., 1992. Radiolarian. In: Yin, H. F., Yang, F. Q., Huang, Q. S., et al., eds., Triassic in Qinling and Adjacent Areas. China University of Geosciences Press, Wuhan. 68–69 (in Chinese)
- Yang, B., Li, H. X., Wignall, P. B., et al., 2019. Latest Wuchiapingian to Earliest Triassic Conodont Zones and $\delta^{13}\text{C}_{\text{carb}}$ Isotope Excursions from Deep-Water Sections in Western Hubei Province, South China. *Journal of Earth Science*, 30(5): 1059–1074. <https://doi.org/10.1007/s12583-019-1018-2>
- Yang, Z. H., Guo, J. F., Su, S. R., et al., 2002. New Advances in the Geological Study of the Qinling Orogen. *Geology in China*, 29(3): 246–256 (in Chinese with English Abstract)
- Yang, Z. H., Chao, H. X., Wu, X., et al., 2016. The Structural Characteristics of Qinling Intra-Continental Orogenic Belt and Its Choula (Drawing-out) Tectonic Orogenic Model. *Earth Science Frontiers*, 23(4): 63–71 (in Chinese with English Abstract)
- Yin, H. F., Yang, F. Q., Lai, X. L., 1988. Triassic Belts and Indosian Development of the Qinling Mountains. *Geoscience*, 2: 355–365 (in Chinese with English Abstract)
- Yuan, J., Jiang, H., Wang, D., 2015. LST: A New Inorganic Heavy Liquid Used in Conodont Separation. *Geological Science and Technology Information*, 34(5): 225–230 (in Chinese with English Abstract)
- Zhang, Z. T., Sun, Y. D., Lai, X. L., 2017. Early Carnian Conodont Fauna at Yongyue, Zhenfeng Area and Its Implication for Ladinian-Carnian Subdivision in Guizhou, South China. *Palaeogeography, Palaeoclimatology, Palaeoecology*, 486(15): 142–157. <https://doi.org/10.1016/j.palaeo.2017.02.011>
- Zhang, Z. T., Sun, Y. D., Lai, X. L., 2018a. Progresses on Carnian (Late Triassic) Conodont Study in Southwest China. *Earth Science*, 43(11): 3955–3975 (in Chinese with English Abstract)
- Zhang, Z. T., Sun, Y. D., Lai, X. L., et al., 2018b. Carnian (Late Triassic) Conodont Faunas from South-western China and Their Implications. *Papers in Palaeontology*, 4(4): 513–535. <https://doi.org/10.1002/spp2.1116>

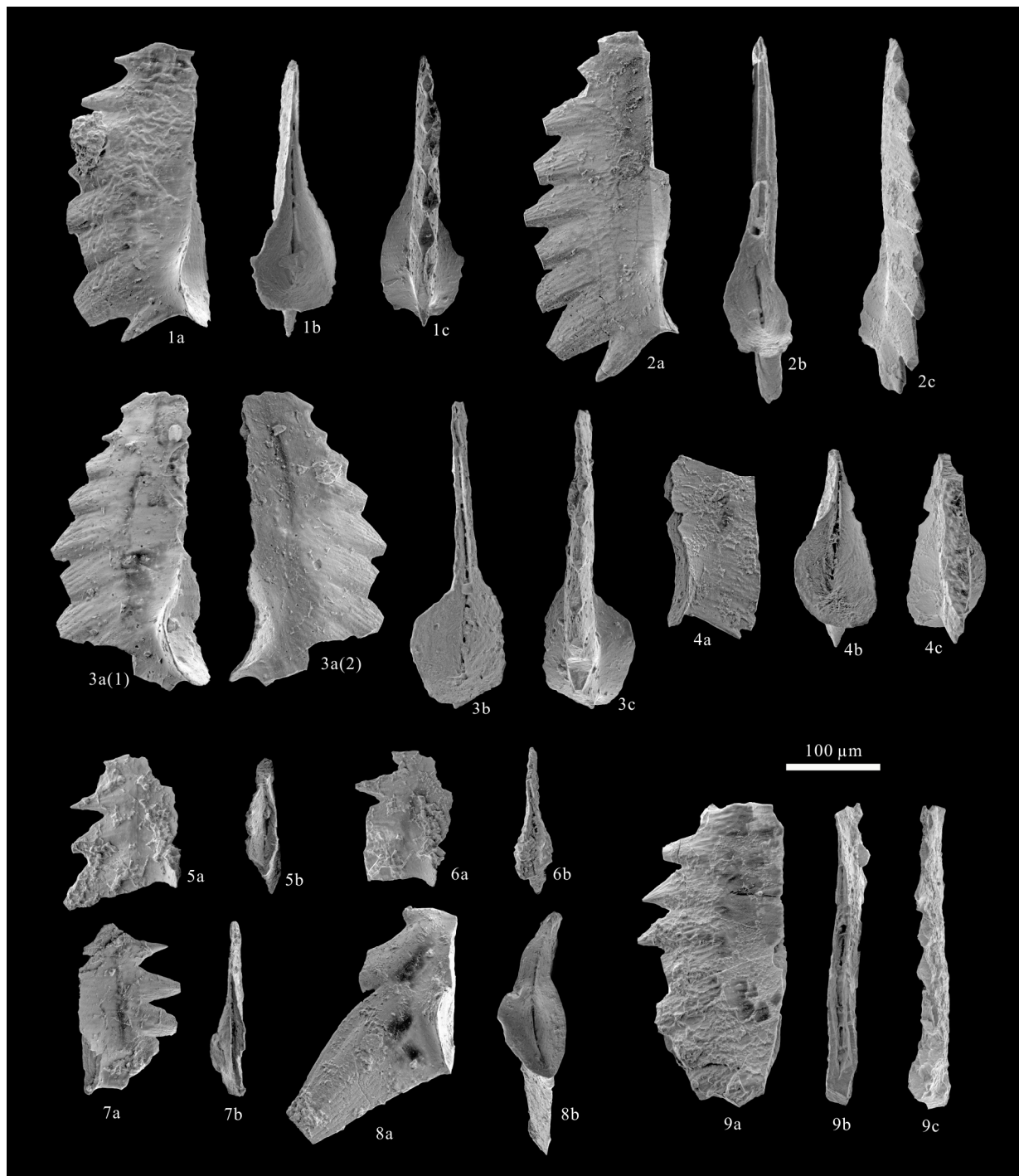


Plate 1. 1–4. *Mosherella longnanensis* sp. nov., registration Nos. DDQ 20032.5001–20032.5004; 5–7. *Mosherella praebudaensis* Chen and Lukeneder, 2017, registration Nos. DDQ 20032.5005–20032.5007; 8. “*Misikella*” *longidentata* Kozur and Mock, 1974, registration Nos. DDQ 20212.8001; 9. *Mosherella* sp., registration Nos. DDQ 20032.5008. a. Lateral view; b. lower view; c. upper view. 1–7, 9 from sample DDQ-32.5, bed 2; 8 from sample DDQ-212.8, bed 10. All are P₁ elements. Scale bar=100 μm. All the specimens are preserved at China University of Geosciences, Wuhan.